

MedChemComm

Accepted Manuscript



This is an *Accepted Manuscript*, which has been through the Royal Society of Chemistry peer review process and has been accepted for publication.

Accepted Manuscripts are published online shortly after acceptance, before technical editing, formatting and proof reading. Using this free service, authors can make their results available to the community, in citable form, before we publish the edited article. We will replace this *Accepted Manuscript* with the edited and formatted *Advance Article* as soon as it is available.

You can find more information about *Accepted Manuscripts* in the [Information for Authors](#).

Please note that technical editing may introduce minor changes to the text and/or graphics, which may alter content. The journal's standard [Terms & Conditions](#) and the [Ethical guidelines](#) still apply. In no event shall the Royal Society of Chemistry be held responsible for any errors or omissions in this *Accepted Manuscript* or any consequences arising from the use of any information it contains.

Paclitaxel loaded human serum albumin nanoparticles stabilized with intermolecular disulfide bonds

Cite this: DOI: 10.1039/x0xx00000x

Shufang Zhao, Wentan Wang, Yanbin Huang*, Yuhang Fu and Yi Cheng*

Received 00th January 2014,
Accepted 00th January 2014

DOI: 10.1039/x0xx00000x

www.rsc.org/

We prepared paclitaxel-loaded disulfide-crosslinked human serum albumin nanoparticles (PTX-HSA-NPs) in a microfluidic platform. The entire process includes four steps, i.e., the pretreatment step to partially reduce albumin, the mixing and co-precipitation step, the reaction step, and the dialysis step. Two important factors dominate the successful preparation of stable PTX-HSA-NPs: one is the choice of the anti-solvent in the co-precipitation step, and the other is the reaction time in the reaction step. We demonstrated that the drug-loaded nanoparticles are stable against dilution by the inter-albumin disulfide bonds, but still have a quick drug release profile in the intracellular-mimicking reduction environment. Through cell studies, we showed that the albumin nanoparticle carriers are safe and characterized the cell toxicity of the paclitaxel-loaded nanoparticles with two relevant cancer cell lines.

Introduction

Paclitaxel (PTX) is a major anticancer drug which is highly efficient in treating many types of cancers. Since it is poorly soluble in water, surfactant and organic solvent (i.e., Cremophor EL (CrmEL) and ethanol) are used in clinical formulation (Taxol®). However, this formulation is toxic and induces hypersensitivity reactions¹. Consequently, various approaches, such as soluble prodrugs², micellar carriers³, liposome carriers, polymer and protein nanoparticles⁴⁻⁶ have been proposed to replace the CremEL/ethanol formation. Among them, albumin based nanoparticle carriers represent an attractive strategy since a significant amount of drug can be incorporated into the particle matrix because of the different drug binding sites in the albumin molecule⁷. Besides, HSA has active targeting ability via gp60 receptor-mediated transcytosis, which may enable tumor targeting⁸. These properties as well as the preferential uptake by tumor cells make HSA an ideal candidate for drug delivery⁹. In the meantime, nanoparticles with the appropriate sizes can also realize the passive targeting effect with enhanced permeability and retention effect (EPR effect) at tumor sites¹⁰, which is of great significance in cancer therapy.

The paclitaxel loaded human serum albumin nanoparticles (PTX-HSA-NPs) need to be stable in the circulation system. The intermolecular disulfide bonds between albumin molecules are the preferred stabilization strategy. It can not only stabilize the NPs against dilution as well as the possible organic solvents during drug loading process, but also make NPs capable of the redox responsiveness in reduction environment. These features allow for the self-cross-linked NPs maintained in blood circulation while degraded by glutathione in the cytoplasm to release drug molecules, and accordingly improve the drug bioavailability.

Many effective technologies for fabricating HSA-NPs and PTX-HSA-NPs have been reported in the literature, such as coacervation, emulsion, and desolvation methods¹¹⁻¹³. Chemically cross-linking agents, such as glutaraldehyde, are often used to stabilize the albumin nanoparticles, but the chemical modification and possible residual aldehyde may cause complications for *in vivo* applications¹⁴. An albumin-based nanoparticle technology was developed to encapsulate lipophilic drugs¹⁵⁻¹⁶. The technology has been applied to fabricate the Nab-paclitaxel (Abraxane) with diameter of 130 nm, which was approved by FDA for clinical treatment of metastatic breast cancer in 2005¹⁷. Although Abraxane is stable as a nanoparticle in its un-diluted formulation, it dissolves rapidly after intravenous infusion which results in soluble albumin-bound paclitaxel complexes having the size of a single albumin¹⁸. Gong et al. developed a denaturation method to prepare albumin nanoparticles by using β -mercaptoethanol (β -ME)⁶. Their nanoparticles were stabilized by hydrophobic association rather than disulfide bonds, and the NPs also dissolved completely even in 15 vol% ethanol/water solutions.

In our previous work¹⁹, we have successfully fabricated the HSA-NPs by a novel self-cross-link strategy without any toxic chemicals. Glutathione (GSH), an endogenous antioxidant *in vivo*, was utilized to break up the intramolecular disulfide bonds, and the intermolecular disulfide bonds in the HSA-NPs are formed in the albumin nano-precipitate via the disulfide-sulfhydryl interchange reaction. We proved that the intermolecular disulfide bond stabilized the obtained HSA-NPs against dilution, while maintained the dissolvability in the physiologically relevant reduction environment. In this study, PTX was entrapped non-covalently in the HSA matrix to form PTX-HSA-NPs in a microfluidic platform. The morphology, physical states and stability of PTX-HSA-NPs were

investigated. The drug release profile and the cytotoxicity of the NPs were also evaluated *in vitro*.

Besides being stable against dilution, the other important property of PTX-HSA-NPs is the control of the particle diameter. The particles need to be long-circulatory without the clearance in blood circulation to achieve the EPR effect for the passive targeting to the tumor sites. Considering the renal clearance, the EPR effect, and the sequestration by the macrophagocytic systems, the ideal size of an engineered long-circulatory particle should be between 10 and 200 nm²⁰. In the desolvation and co-precipitation process of the PTX-HSA-NPs, the mixing efficiency of the solvents is predominant to determine the average diameter and size distribution of the resultant nanoparticles. Previous studies were done with macroscopic mixers, where the rate of the anti-solvent addition was adjusted to control the nanoparticle sizes^{13, 21}. Droplet-based microfluidic system has been developed very fast in recent years because of its excellent mass and heat transfer performance and the flexibility to control the reaction process inside each droplet²². It has been indicated in our previous work that the mixing inside the micro-droplet reactor can be completed in a very short flow distance by the direct measurement results via μ -LIF method²³. The preparation of curcumin nanoparticles also demonstrated the necessity of the high mixing efficiency during the desolvation step very well, which could be realized by a micro-droplet reactor in a gas-liquid segmented micro-flow. In this study, a similar microfluidic platform was adopted to replace the traditional batch reactor.

Experimental setup

The experimental procedure is shown in Fig.1. Firstly, in the pretreatment step, HSA was incubated in deionized water with GSH to partially reduce the 17 intramolecular disulfide bonds to free sulfhydryl groups. Then, the solution was dialyzed at 4 °C with deionized water to remove the excessive GSH (membrane cutoff MW: 12-14K Dalton). Then, in the mixing and co-precipitation step, the pretreated 40 mg·mL⁻¹ HSA/water

solution was mixed with the PTX/TBA (holding the input ratio of HSA to PTX constant at 5:1,w/w), only changing the volume of TBA (tertiary butyl alcohol) in a microchannel reactor with a flow condition of $Re = 15$ and $Q_G = 3 \text{ mL} \cdot \text{min}^{-1}$ at 37 °C, using TBA as the anti-solvent for albumin and water as the anti-solvent for paclitaxel. The microchannel used here was similar to the one in our previous work²³, i.e., a traditional Y mixer with three liquid inlets and an additional air inlet to form a segmented gas-liquid flow. Microfluidic platform provided a better controlled mixing performance, resulting in supersaturation for both albumin and the drug which is crucial in the preparation of the NPs with narrow size distribution²³⁻²⁴. Due to the huge decrease of the solubility of both PTX and HSA in the mixed solution, they would precipitate out together and assemble into PTX-HSA-NPs in the rapid mixing process. Afterwards, in the reaction step, the suspension was incubated at 37 °C to form intermolecular disulfide bonds through the disulphide-sulfhydryl interchange reaction¹⁹. After that, the suspension was dialyzed against deionized water at 4 °C to remove the TBA (membrane cutoff MW: 12-14K Dalton). The obtained PTX-HSA-NPs was stored as a suspension at 4 °C for short-term storage or as powders at -20 °C after freeze drying process for long-term preservation.

Scanning and Transmission electron microscopy (JSM-7401 and JEM-2010, JEOL Ltd., Japan) were used to characterize the morphology of the PTX-HSA-NPs. Average particle size was measured by phase analysis light scattering (PALS) using ZetaPALS, Zeta Potential Analyzer (Brookhaven Instruments Corp., USA). The samples were diluted with deionized water and measured at 25 °C and scattering angle of 90°.

The total PTX loading content (% w/w) was defined as (PTX weight in powder/total powder weight) × 100%, while PTX entrapment efficiency of the fabrication process was defined as PTX yield (% w/w) = (PTX weight in powder/total input of PTX) × 100%. To determine the loading content of PTX, the original PTX-HSA-NPs suspension and the supernatant were diluted in 2 mL of acetonitrile (19:1, v/v) and sonicated for 30 min to extract PTX completely.

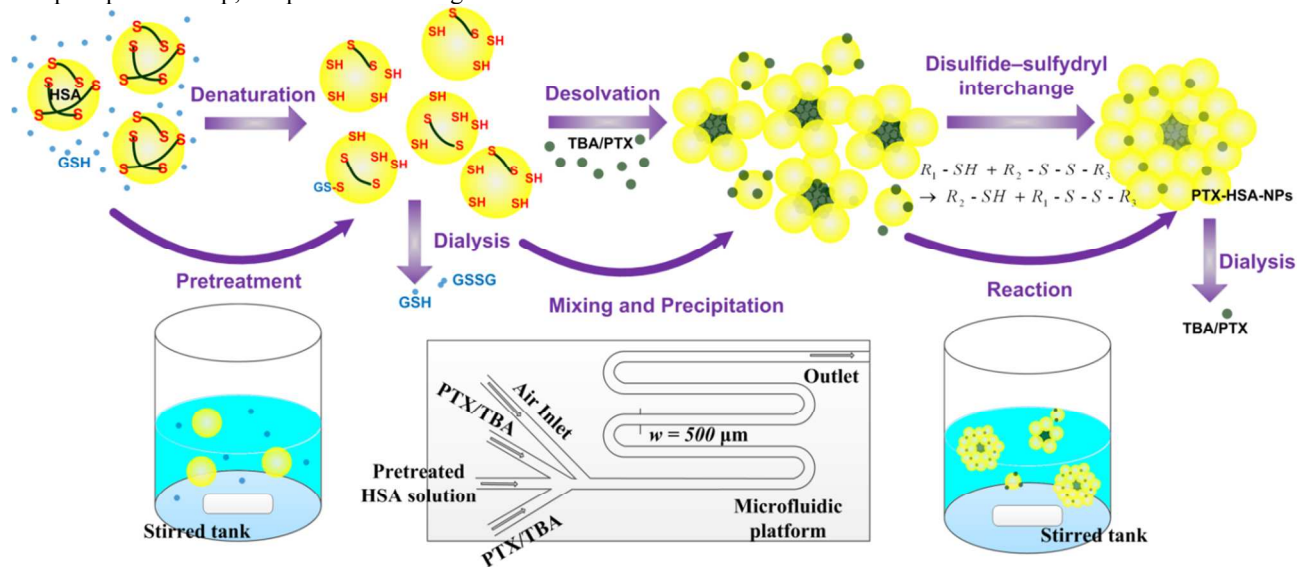


Fig. 1 The scheme and procedure of the preparation of PTX-HSA-NPs.

PTX levels were determined by high-performance liquid chromatography (HPLC) using a VP-ODS C18 column (150 mm×4.6 mm, 5 μm particle size) at 30 °C. The mobile phase consisted of 20% methanol, 50% acetonitrile and 30% water. The system was run at a flow rate of 0.7 mL·min⁻¹ and PTX was detected at 228 nm.

In the products, both HSA and PTX exist in two forms: the nanoparticles and the free ones. For the determination of free HSA molecules remained in solution, the NPs were separated from the supernatant by centrifugation at 16,000 × g at 4 °C for 20 min. An aliquot of the supernatant (0.1 mL) was diluted ten times and the amount of the dissolved HSA was determined using the Bradford method as previously described¹⁹. The free PTX is defined as the amount of PTX in the supernatant after the centrifugation.

To determine the PTX release profile, 0.5 mL PTX-HSA-NPs suspension was placed into a dialysis bag (membrane cutoff MW: 1000 Dalton) under the same content of NPs (the reference content is the amount of HSA). Then the bag was immersed into 50 mL release solution (PBS buffer with/without 10 mM GSH). At certain time points, 1 mL release solution was withdrawn for UV/VIS spectrophotometer analysis, and same volume of release solution was added.

The cytotoxicity of PTX-HSA-NPs was assessed with cell line of human breast cancer cells (MCF-7), purchased from the Chinese Academy of Science, Shanghai, China. The cell line was characterized according to the guidelines issued by ATCC. Cells were maintained in DMEM media, supplemented with 10% (v/v) FBS (fetal bovine serum) containing 1% penicillin/streptomycin in a 5% CO₂ humidified atmosphere at 37 °C. For dose-dependent cytotoxicity assays, cells were seeded in 96-well plates at 5×10³ cells/well and pre-incubated for 24 h. Media were replaced with fresh serum-free DMEM and then pre-set amounts of different drug forms were added and incubated for 72 h. The *in vitro* cytotoxicity of PTX-HSA-NPs, PTX suspension in HSA solutions (PTX/HSA ratio was kept constant at 1:8, w/w), Taxol-mimicking formulation (i.e. Cremophor-EL and ethanol, 1:1 v/v) and HSA-NPs were determined using MTT assays. The cell viabilities were calculated by the ratio of absorbance of test cells and that of control cells, and the control groups were set as 100%.

Results and discussion

In our previous work¹⁹, we have fabricated HSA-NPs which were stabilized with the reversible inter-albumin disulfide bonds by using the desolvation method. Here PTX was added into the system and co-precipitated with the albumin, and finally obtained PTX-loaded HSA-NPs. A microchannel mixer was used to control the rapid mixing process of HSA/water solution and PTX/organic solvent solution. The HSA and PTX precipitated out together to form the PTX-HSA-NPs, instead of forming precipitates separately. Two factors are crucial to obtain the stable PTX-HSA-NPs with high quality: one is choosing the anti-solvent in the precipitation step, and the other is controlling the reaction time in the reaction step.

There are two frequently-used organic solvents as the anti-solvent to water, i.e. ethanol and tertiary butyl alcohol (TBA), which were used in the production process of food and pharmaceuticals. Both of the two solvents worked well in the preparation of PTX-HSA-NPs during mixing and reaction steps. However, different results turned out after the dialysis process. Fig. 2a and 2b show the SEM pictures of the particles before and after the dialysis process with ethanol as the anti-solvent,

while Fig. 2c and Fig. 2d show the SEM and TEM pictures of the products after the dialysis process with TBA as the anti-solvent. It can be clearly seen that the product with ethanol shows needle crystals of paclitaxel (Fig. 2b) while the product with TBA results in spherical nanoparticles with the paclitaxel in the amorphous state (as shown by the electron diffraction in Figure 2d). The particles in Fig. 2a seem to be embedded in a layer of thin films. We have analyzed the composition of the mixed solution with ethanol as the anti-solvent after mixing and reaction steps. The results show that 90% of the PTX still remained in the solution, which means only a small amount of PTX has been embedded into the nanoparticles. The particles in Fig. 2a are mostly HSA-NPs with a small amount of PTX content. With continuous dialysis of ethanol and the transmembrane transport of the ethanol and PTX at different speed, the solubility of PTX in the solution becomes lower and lower, which results in the recrystallization of PTX into needle crystals. We have also analyzed the composition of the mixed solution with TBA as the anti-solvent after mixing and reaction steps. Although the results also show that 50% of the PTX remained in the solution, the free PTX can be dialyzed out with TBA instead of recrystallization in the dialysis bag. If we adjust the volume ratio of solvents and use less ethanol to reduce the solubility of PTX, the solubility of HSA in the mixed solution will be increased and the co-precipitation would not occur. Thus, considering the appropriate solubility of both HSA and PTX, TBA is a better choice in our process.

Then, we investigated the influence of the reaction time (cases 1, 2, 3 and 4 represent the reaction times of 8, 15, 25 and 35 min, respectively) and the ratio of organic solvent/water on the stability and physical states of PTX-HSA-NPs.

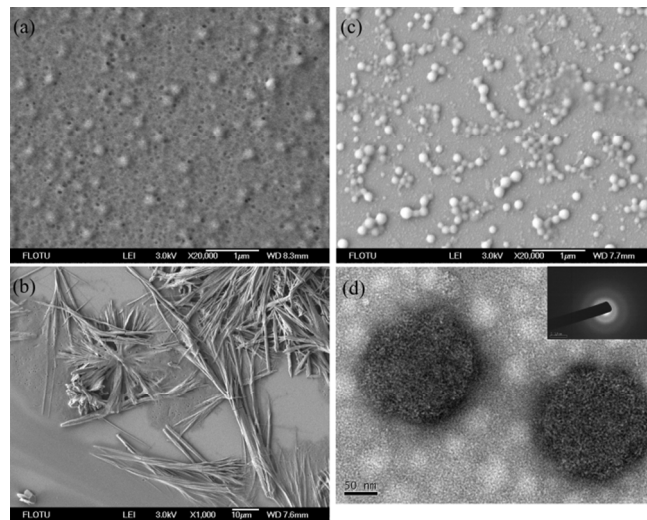


Fig. 2 SEM and TEM results of PTX-HSA-NPs. (a) and (b) SEM result with ethanol as anti-solvent. (c) SEM result with TBA as anti-solvent. (d) TEM result with TBA as anti-solvent.

Fig. 3a shows the stability of the PTX-HSA-NPs with different reaction times against dilution (with final concentration of NPs about 0.2 mg·mL⁻¹) in the phosphate buffer solutions. Firstly, the NPs with longer reaction time have smaller diameters. The reason is probably attributed to that it takes time for each particle to form the intermolecular disulfide bonds inside through the disulphide-sulfhydryl interchange reaction, though the NPs precipitate out immediately after the mixing of two solutions. A shorter reaction time means fewer

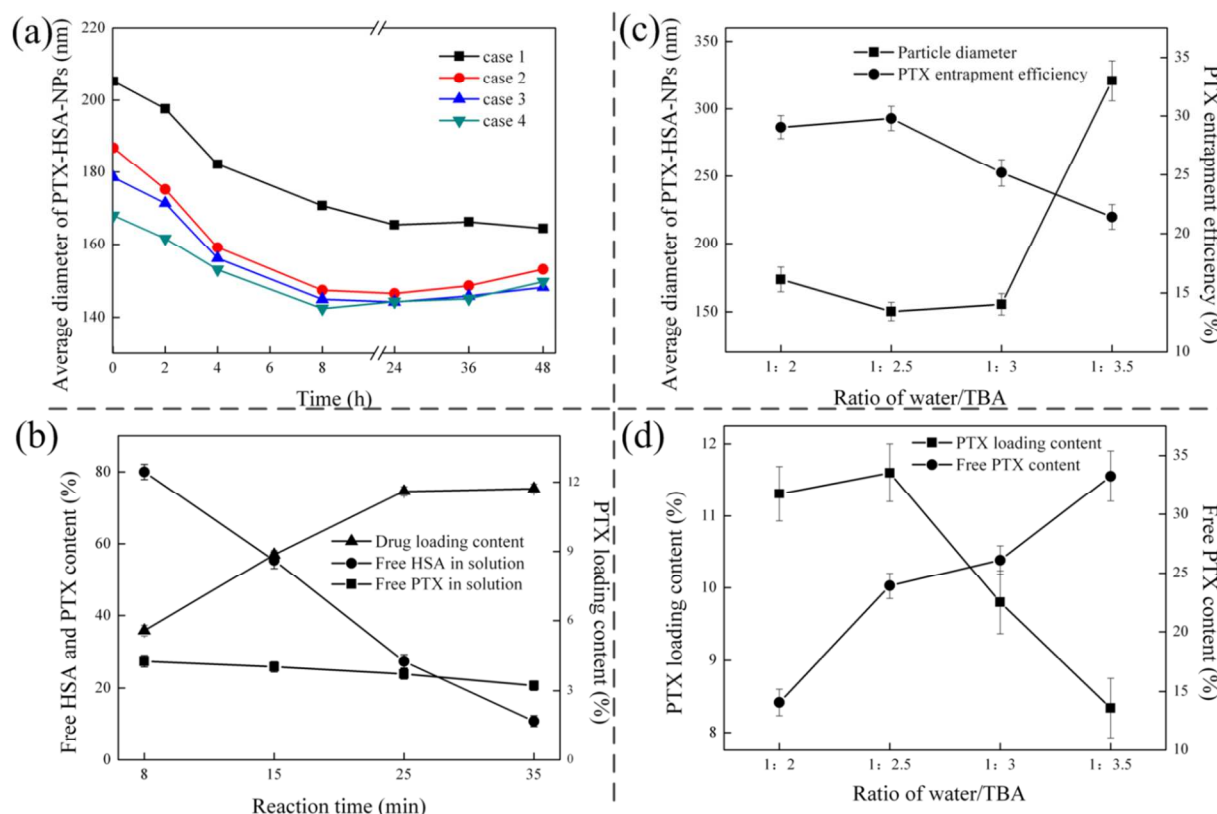


Fig. 3 Stability and physical states of PTX-HSA-NPs. (a) Stability of the PTX-HSA-NPs with different reaction times. (b) Amount of free HSA and PTX molecules in the suspension. (c) Influence of the ratio of water/ TBA on the diameter of PTX-HSA-NPs and yield of PTX. (d) Influence of the ratio of water/ TBA on the PTX loading content and the content of free PTX.

intermolecular disulfide bonds, resulting in loose structure and a smaller amount of stable NPs, which leaves more free PTXs and HSAs in the solution. Those NPs with a sufficient reaction time will have enough intermolecular disulfide bonds inside to make a tighter structure and leave fewer free HSAs and PTXs in the solution, which results in a smaller diameter. We can also see it from Fig. 3b, which represents the PTX loading content and the amount of free HSA and PTX molecules in the suspension after the dialysis step. With the increasing of reaction time, the free HSA molecules in the solution decrease from 80% to 15%, which means the formation of more intermolecular disulfide bonds to make the HSA molecules link to each other inside the NPs. Meanwhile, PTX loading efficiency increases from 5% to 11%, and the free PTXs, which bind to the free HSA molecules in the solution, remain around 25% with a slight decrease. Besides, all the obtained NPs shrank to certain extent in the first several hours of dilution and then remained stable for at least 48 hours, all in the range of 140-180 nm. It is probably because that when diluted in PBS buffer, the environment of the particles changed from pure water (after dialysis) to a salt solution, and this resulted in size adjustment of these nanoparticles.

Fig. 3c and Fig. 3d show the influence of the ratio of water/ TBA on the physical states of PTX-HSA-NPs with a reaction time of 25 min based on the same amount of PTX input. The PTX entrapment efficiency decreases with the increased use of TBA (Figure 3c). This result is understandable because the increase of TBA will increase the solubility of the PTX in the TBA/water solution, which results in a lower loading content and yield of PTX. For the same reason, as more TBA is used,

the drug loading decreases and the percentage of free PTX in the solution increases (Figure 3d). The diameters of the NPs are more or less the same around 160 nm at the water/TBA ratios of 2, 2.5 and 3, but it increases up to 300 nm when the ratio exceeds 3 (Figure 3c). When the ratio is less than 2, a significant amount of HSA molecules will be soluble in the mixed solution. From the above results, with the optimal protocol (TBA as the anti-solvent, water/TBA ratio 2.5, and 25 min reaction), we can obtain stable PTX-HSA-NPs with 160 nm diameter and a total 11% PTX loading, 75% of which inside the NPs and 25% of PTX combined with free HSA molecules.

Fig. 4 shows the *in vitro* PTX release profiles of obtained PTX-HSA-NPs in different PBS buffer solution at 30 °C. We use PBS buffer at pH 7.4 without reductant and PBS buffer at pH 5.5 with 10 mM GSH to mimic the extracellular condition and the endosome/lysosome environment, respectively. Fig. 4a shows the *in vitro* release profiles of the NPs prepared at different reaction times. The release profiles in the reduction environment indicate a relatively rapid drug release in the initial 12 hours while the release profiles in the non-reduction environment are approximate an asymptotic release which is the typical pattern of PTX-loaded nanoparticles in the literature^{5, 25-26}. PTX-HSA-NPs made with the least reaction time have the highest release rate because it has less intermolecular disulfide bonds and PTX content.

We further investigate the release behavior of case 3 in the PBS buffer with/without the reductant at different pH values, as shown in Fig. 4b. The results show that the PTX releases faster at a higher pH value in the reduction environment probably due to the stronger reduction capacity of GSH in the alkaline

environment, but the release is complete after 24 hours at both pH 5.5 and 7.4. The results in the non-reduction environment are just the opposite: the PTX releases faster at a lower pH value. It may be because the different conformation of HSA molecule in different pH environments: HSA in acid environment is in a more expanded conformation and this may result in a faster release of the bound drugs⁷.

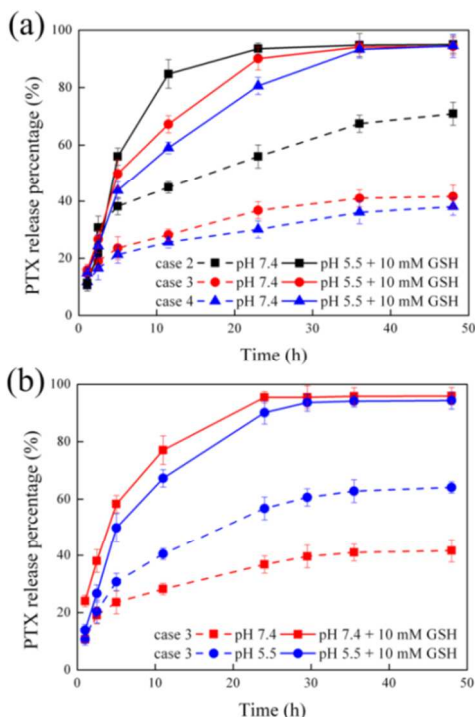


Fig. 4 Drug release profiles of PTX-HSA-NPs. (a) Release profiles of the NPs prepared under different reaction times. (b) Release behavior of case 3 in the PBS buffer with/without the reductant at different pH values.

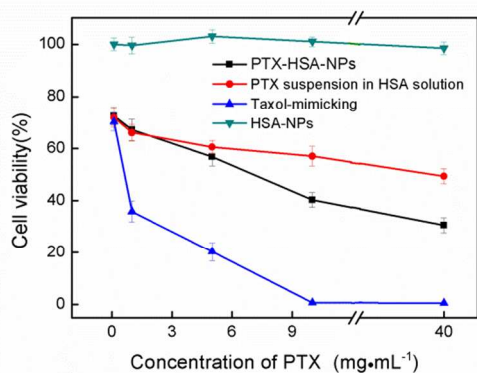


Fig. 5 In vitro cytotoxicity of different types of drug forms (PTX-HSA-NPs, PTX suspension in HSA solution, Taxol-mimicking formulation and HSA-NPs) on human breast cancer cells (MCF-7).

The cytotoxicity of PTX-HSA-NPs was investigated using MCF-7 cells, in comparison with PTX suspension in HSA solution, Taxol-mimicking formulation and HSA-NPs, as shown in Fig. 5. The IC₅₀ value (inhibitory concentration of 50%) of PTX-HSA-NPs against MCF-7 cells is about 7.8 μg·mL⁻¹. The cytotoxicity of our PTX-HSA-NPs against MCF-7 is similar to the result in the literature, for example, IC₅₀ = 9.4 μg·mL⁻¹ against MCF-7 by PTX loaded PCL-TPGS

nanoparticles²⁷. This value is higher than that of the Taxol-mimicking formulation but lower than that of the PTX suspension group. Also, the results show that the drug-free HSA-NPs do not have noticeable cytotoxicity, i.e., the HSA-NPs are safe and suitable as a drug carrier for therapeutic applications.

Conclusions

In this work, we used a microfluidic mixer and a coprecipitation method to fabricate the PTX-HSA-NPs. The obtained PTX-HSA-NPs have the intermolecular disulfide bond to stabilize themselves against dilution. Two key factors dominate the preparation of these stable PTX-HSA-NPs: one is the choice of the anti-solvent in the precipitation step, and the other is the reaction time in the reaction step. The morphology, physical states and stability of PTX-HSA-NPs are well investigated. The results show that with the optimal protocol (TBA as the anti-solvent, water/TBA ratio 2.5, and 25 min reaction time), we can obtain stable PTX-HSA-NPs with a diameter around 160 nm and a total 11% PTX loading, which has 75% of PTX inside the NPs and 25% of PTX combined with free HSA molecules around. The final PTX concentration in the suspension is about 420 μg/ml. The total concentration of PTX plus HSA in the suspension is about 3.6 mg/ml. The cross-linked PTX-HSA-NPs are stable and have a slow PTX release profile in the PBS buffer (pH 7.4), while they have the redox responsiveness with a quick PTX release in the physiologically relevant reducing environment. The results of biological cytotoxicity show that the obtained PTX-HSA-NPs are a safe nano-carrier system for therapeutic applications. We believe that the present method can be generalized to other anticancer drugs (e.g. curcumin) to form the platform nano-carrier system for the drug delivery and tumor targeting.

Acknowledgements

This study is supported by National 973 Project of PR China (No. 2013CB733604).

Notes and references

* Department of Chemical Engineering, Tsinghua University, Beijing 100084, P. R. China. Fax: 86-10-62772051; Tel: 86-10-62797572 (Y.H.) and 86-10-62794468 (Y.C.); E-mail: yanbin@tsinghua.edu.cn (Yanbin Huang) and yicheng@tsinghua.edu.cn (Yi Cheng)

- 1 T. E. Stinchcombe, *Nanomedicine*, 2007, **2**, 415.
- 2 M. Skwarczynski, Y. Hayashi, and Y. Kiso, *Journal of Medicinal Chemistry*, 2006, **49**, 7253.
- 3 W. Y. Seow, J. M. Xue, and Y. Y. Yang, *Biomaterials*, 2007, **28**, 1730.
- 4 E. A. Ho, V. Vassileva, C. Allen, and M. Piquette-Miller, *Journal of Controlled Release*, 2005, **104**, 181.
- 5 D. M. Zhao, X. H. Zhao, Y. G. Zu, J. L. Li, Y. Zhang, R. Jiang, and Z. H. Zhang, *International Journal of Nanomedicine*, 2010, **5**, 669.
- 6 G. M. Gong, Y. Xu, Y. Y. Zhou, Z. J. Meng, G. Y. Ren, Y. Zhao, X. Zhang, J. H. Wu, and Y. Q. Hu, *Biomacromolecules*, 2012, **13**, 23.
- 7 T. Peters, *Advances in Protein Chemistry*, 1985, **37**, 161.
- 8 S. A. Rempel, S. G. Ge, and J. A. Gutierrez, *Clinical Cancer Research*, 1999, **5**, 237.
- 9 F. Kratz, *Journal of Controlled Release*, 2008, **132**, 171.

- 10 H. Maeda, J. Wu, T. Sawa, Y. Matsumura, and K. Hori, *Journal of Controlled Release*, 2000, **65**, 271.
- 11 W. Lin, A. G. A. Coombes, M. C. Davies, S. S. Davis, and L. Illum, *Journal of Drug Targeting*, 1993, **1**, 237–243.
- 12 B. G. Muller, H. Leuenberger, and T. Kissel, *Pharmaceutical Research*, 1996, **13**, 32.
- 13 K. Langer, S. Balthasar, V. Vogel, N. Dinauer, H. von Briesen, and D. Schubert, *International Journal of Pharmaceutics*, 2003, **257**, 169.
- 14 W. Fürst and A. Banerjee, *Annals of Thoracic Surgery*, 2005, **79**, 1522.
- 15 N. P. Desai, C. Tao, A. Yang, L. Louie, Z. Yao, P. Soon-Shiong and S. Magdassi, *U.S. Patent*, 1999, No. 5916596.
- 16 N. P. Desai, P. Soon-Shiong, *U.S. Patent*, 2004, No. 6753006B1.
- 17 N. Desai, V. Trieu, Z. W. Yao, L. Louie, S. Ci, A. Yang, C. L. Tao, T. De, B. Beals, D. Dykes, P. Noker, R. Yao, E. Labao, M. Hawkins, and P. Soon-Shiong, *Clinical Cancer Research*, 2006, **12**, 1317.
- 18 B. Elsadek and F. Kratz, *Journal of Controlled Release*, 2012, **157**, 4.
- 19 W. T. Wang, Y. B. Huang, S. F. Zhao, T. Shao, and Y. Cheng, *Chemical Communications*, 2013, **49**, 2234.
- 20 S. M. Moghimi, A. C. Hunter, and J. C. Murray, *Pharmacological Reviews*, 2001, **53**, 283.
- 21 M. Wacker, A. Zensi, J. Kufleitner, A. Ruff, J. Schutz, T. Stockburger, T. Marstaller, and V. Vogel, *International Journal of Pharmaceutics*, 2011, **414**, 225.
- 22 H. Song, D. L. Chen, and R. F. Ismagilov, *Angewandte Chemie-International Edition*, 2006, **45**, 7336.
- 23 S. F. Zhao, W. T. Wang, T. Shao, M. X. Zhang, Y. Jin, and Y. Cheng, *Chemical Engineering Science*, 2013, **100**, 456.
- 24 F. S. Majedi, M. M. Hasani-Sadrabadi, S. H. Emami, M. A. Shokrgozar, J. J. VanDersarl, E. Dashtimoghdam, A. Bertsch, and P. Renaud, *Lab on a Chip*, 2013, **13**, 204.
- 25 K. M. Huh, H. S. Min, S. C. Lee, H. J. Lee, S. Kim, and K. Park, *Journal of Controlled Release*, 2008, **126**, 122.
- 26 L. Q. Jiang, Y. S. Xu, Q. Liu, Y. Tang, L. Ge, C. L. Zheng, J. B. Zhu, and J. P. Liu, *International Journal of Pharmaceutics*, 2013, **443**, 80.
- 27 E. Bernabeu, G. Helguera, M. J. Legaspi, L. Gonzalez, C. Hocht C, Taira, D. A. Chiappetta. *Colloids and Surfaces B: Biointerfaces*, 2014, **113**: 43-50.

Graphical Abstract

A self-cross-link strategy was adopted to form inter-protein disulfide crosslinks with albumin's own thiol groups. PTX was further entrapped non-covalently in HSA matrix to form paclitaxel loaded HSA nanoparticles (PTX-HSA-NPs).

